An *ab initio* study of optical and Raman spectra of heavily Li-doped 4 Å carbon nanotubes

2004 J. Phys.: Condens. Matter 16 1467

(http://iopscience.iop.org/0953-8984/16/8/027)

INSTITUTE OF PHYSICS PUBLISHING JOURNAL OF PHYSICS: CONDENSED MATTER

J. Phys.: Condens. Matter **16** (2004) 1467–1488 PII: S0953-8984(04)71815-9

An *ab initio* study of optical and Raman spectra of heavily Li-doped 4 Å carbon nanotubes

B K Agrawal, S Agrawal and Rekha Srivastava

Physics Department, Allahabad University, Allahabad 211002, India

Received 11 November 2003
Published 13 February 2004
Online at stacks.iop.org/JPhysCM/16/1467 (DOI: 10.1088/0953-8984/16/8/027)

Abstract

An extended and systematic *ab initio* investigation of the energetics, structural, electronic, optical and Raman-active properties of heavily Li-doped ultrathin 4 Å diameter carbon nanotubes of different chiralities has been performed. A number of new features not discussed earlier are observed in the present study. Our values for the binding energies of the Li-doped tubes are higher than the ones reported earlier. We find the Li-doped (3, 3) tubes stable in contrast to an earlier prediction. For each type of the tube, the saturation intake of Li atoms inside the tube is 8–10% only, whereas on the surfaces of the (5, 0) and (4, 2) tubes, this intake is as high as 100%, and it forms a circular tube of Li^+ ions around the tube.

Li atoms residing on the axis inside the tube do not modify the symmetry of the host tube and thus the electronic structure (except the upward shifting of the Fermi surface, E_F) in contrast to surface Li atoms which (apart from the (4, 2) tube, which possesses no symmetry) destroy the symmetry and drastically alter the electronic structure. In general, Li doping inside or outside the tube increases the electron density of states (DOS) several times except in the (5, 0) tube doped with a small concentration of Li atoms, where it decreases. For one inner Li atom in each tube, the peak structure in the optical absorption remains essentially the same as that of the pristine tube. In general, the optical absorption is different for the various nanotube–Li configurations studied.

For each type of tube, in general, the RBM frequency reduces with the dilation of the diameter of the optimized tube. The high values of DOS obtained for certain Li concentrations may lead to high values of electrical conductivity and the superconducting transition temperatures in Li-doped tubes as has already been reported in pristine tubes and ropes.

1. Introduction

The unique properties of the carbon nanotubes are small diameter, high tensile strength, (Tu and Ou-Yang 2002), high chemical and thermal stabilities, and remarkable electronic conduction (Baughman *et al* 2002, Yoon *et al* 2002, Farajian *et al* 2003). The novel properties

of these tubes stem both from their quasi-one-dimensional character as well as from the smallness of their diameters. Efforts have thus been made to achieve the smallest possible diameter nanotubes whose behaviour may be quite different from that of comparatively large diameter ones because of the strong curvature effects. The simple band-folding picture of a graphene sheet will not be valid. Recently, small 4 Å single walled nanotubes (SWNT) have been synthesized (Qiu *et al* 1989, Tang *et al* 1998, Qin *et al* 2000, Wang *et al* 2000). Much progress has been made in the synthesis of 4 Å SWNTs inside the microporous zeolite $AlPO_{4-5}$ (AFI) (Shimoda *et al* 2002). The tubes are mono-sized and are arranged in a close-packed hexagonal lattice. They have been well characterized by transmission electron microscopy (Tang *et al* 1998, Wang *et al* 2000, Liang *et al* 2002), x-ray diffraction (Launois *et al* 2000), optical absorption and Raman data (Sun *et al* 1999, Moli *et al* 2001, Lie *et al* 2001, Jorio *et al* 2002, Liang *et al* 2002). Quite recently, one-dimensional superconducting fluctuations with a mean-field T_c of 15 K in 4 Å SWNTs have been reported (Tang *et al* 2001).

In one-dimensional systems like nanotubes, there appear van Hove singularities (vHs) at the centre and the boundary of the Brillouin zone (BZ) and the saddle points within the BZ. These critical points lead to square-root-like singularities in the electron density of states (DOS). Scanning tunnelling measurements have revealed such singularities (Qiu *et al* 1989, Launois *et al* 2000) on the top of the ropes of both the armchair and zigzag nanotubes. Ouyang *et al* (2001) had shown the occurrence of small gaps using scanning tunnelling microscope. Other methods such as optical absorption and Raman scattering have also been employed to study the electronic structure of the nanotubes. Up to now, most of the efforts have been concentrated on nanotubes having large diameters >7 Å and only some studies are available for the smallest nanotubes of diameter 4 Å.

The study of carbon nanotubes doped with atoms or molecules of different kinds is of utmost importance for their future potential applications especially in gas storage (Schlapbach and Zuttel 2001, Hirscher *et al* 2002), field emission (Saito *et al* 2002), biotechnology (Shim *et al* 2002), electronic and thermal properties (Kong *et al* 2000, Collins *et al* 2002, Sumanasekera *et al* 2000) and also as templates for the preparation of one-dimensional alkali or metallic nanowires and nanotubes, etc.

Doping the carbon nanotubes with Li is more attractive as the nanotube may be used as an efficient anode material for rechargeable Li-ion batteries. A reversible lithium storage capacity increase from LiC_6 to LiC_3 has been achieved by chemical etching of nanotubes to short segments (Shimoda *et al* 2002).

Li, being a small atom, is quite favourable thermodynamically and kinetically to be doped in small diameter nanotubes. Bendiab *et al* (2001) studied the absorption and Raman spectrum of films of Li_x C compounds ($0 \leqslant x \leqslant 0.17$) in wide tubes of diameters 12–16 Å of different chiralities. Very recently, Ye *et al* (2003) measured the resonant Raman spectrum of Li-doped 4 Å SWNTs and showed enhancement of the radial breathing mode (RBM) frequency and softening of the G-band. On the theoretical side, Zhao *et al* (2000) studied the electronic structure and the energy of Li-intercalated wide tubes. Liu and Chan (2003) have investigated the energetics and electronic structure of 4 Å nanotubes with different chiralities doped with different concentrations of Li in the low-concentration limit.

A doped Li atom may reside at different locations of the nanotubes: inside the tube at different positions, and at various sites on the surface of the tube like above the centre of the hexagon of C atoms (mid-hexagon) or above the mid-points of the C–C bonds. The doped Li atom concentrations may also vary. What are the saturating Li concentrations for the stabilized configurations? How do these Li atoms affect the electronic structure, the electromagnetic absorption and Raman scattering, etc, and how may the experimental techniques be utilized to detect the locations of Li atoms and their concentrations? All the above questions need

to be understood for the future technological applications of Li-doped nanotubes. The above questions have been addressed in the present paper.

In the present study, we investigate the stability, electronic structure, optical absorption and Raman scattering of 4 Å SWNTs of different chiralities in the high-concentration limit of Li doping. Most of our results are in agreement with Liu and Chan (2003) in the dilute Li concentration limit apart from striking differences in the stabilities of the optimized structures.

2. Method and technical details

The calculations have been performed in a self-consistent manner using the ABINIT[1] (UCLCI Project) code which uses pseudopotential and the plane waves along with density functional theory. An efficient fast Fourier transform algorithm (Goedecker 1997) is used for the conversion of the wavefunctions between the real and reciprocal lattices. The wavefunctions are determined in a fixed potential according to a state by state or band by band conjugate gradient algorithm (Payne *et al* 1992, Gonze 1996). A self-consistent potential is determined by using a potential-based conjugate gradient algorithm. We consider a soft non-local pseudopotential of Troullier and Martins (1991) within a separable approximation (Kleinman and Bylander 1982) and use the exchange correlation potential of Perdew *et al* (1996) in generalized gradient approximation (GGA) generated by FHI code (Fuchs and Scheffler 1999). The above method has been successfully applied for the study of wide (6, 6) nanotube and their ropes by the present authors (Agrawal *et al* 2003).

All the structures have been optimized to achieve minimum energy by relaxing both the lattice constants and the atomic positions in the unit cell simultaneously. It may be pointed out that the binding energy and magnitude of atomic relaxation depend on the plane wave cut-off energy, and one should obtain convergence with respect to the cut-off energy too.

The calculations have been performed in a self-consistent manner. In general, the studied structures have been optimized for Hellmann–Feynman forces as small as 10^{-2} eV Å^{-1} on each atom except in some cases where the forces are higher but less than 10^{-1} eV Å^{-1}. Sufficient vacuum space has been chosen to avoid the interference effects between neighbouring isolated nanotubes in supercell geometries. A cut-off energy of 60 Ryd for the plane wave basis has seen to be sufficient for achieving convergence.

3. Calculation and results

3.1. Structural properties

There are three types of 4 Å diameter nanotubes: two achiral (the armchair (3, 3) and the zigzag (5, 0)) and one chiral (4, 2). The diameters of the undoped (3, 3), (5, 0) and (4, 2) nanotubes are 4.21, 4.09 and 4.29 Å, respectively.

For establishing the stability of a configuration, we define the binding energy (BE) of the system by subtracting the optimized energy of the unit cell of the doped nanotube from the sum of the optimized energy of the unit cell of the undoped nanotube and the energies of the isolated Li atoms taken in the unit cell of the doped tube, and divide the difference by the number of Li atoms. The BE is thus the gain in energy of the configuration per Li atom. The Li atoms per unit cell give rise to infinitely extended monoatomic straight chains of Li ions parallel to the tube axis inside or outside it. The nanotube thus works as a template for the creation of linear/zigzag chains or circular tubes of Li atoms.

[1] ABINIT code is a common project of the Université Catholique de Louvain, Corning Inc. and other contributors.

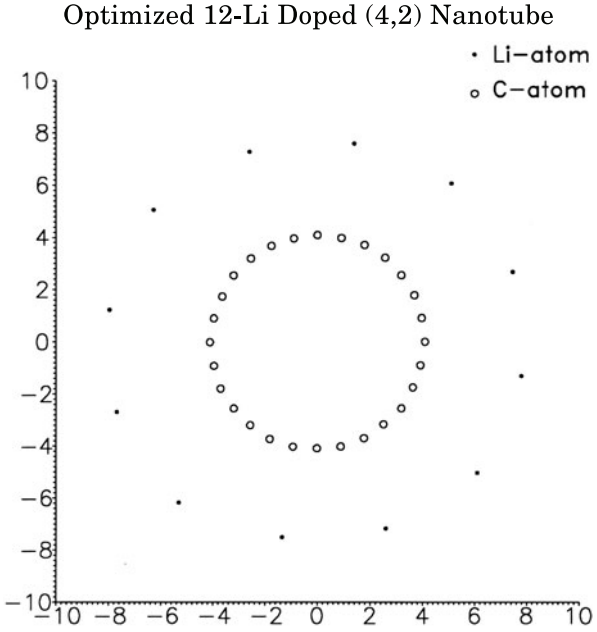

Figure 1. The atomic configuration of an optimized (4, 2) nanotube doped with 12-Li atoms on the surface lying in a plane normal to the tube axis.

We have considered all the various stable configurations of the nanotube plus one or more than one Li atom per unit cell both inside and outside the tubes, separately. The number of Li atoms saturating the intake of the Li atoms depends on the particular tube. The various locations of the Li atoms inside the tube are 1- or 2-Li atoms on the tube axis lying within planes of the carbon atoms or between the adjacent planes of the carbon atoms. The Li atoms lying on the axis of the tube do not change the point-group symmetry of the host. On the surface of the tubes, the studied sites are Li residing above the mid of the C–C bonds or at the centre of the hexagon formed by six C-atoms (mid-hexagon). On the other hand, the Li atoms lying on the surface of the tube change the point-group symmetry of the host. As a typical case, we depict a (4, 2) nanotube doped with 12-Li atoms lying on the surface of the tube in a plane normal to the tube axis in figure 1.

We have investigated the plane wave cut-off energy dependence of the BEs for tubes doped with different numbers of Li atoms and find that the BEs are cut-off energy independent above a cut-off energy of 20 Ryd for the (3, 3) and (5, 0) nanotubes but above a cut-off energy of 60 Ryd for the (4, 2) tube. The BEs converge to fixed values above these cut-off energies for the plane waves.

The BEs for the various locations of the Li atoms inside or outside the nanotubes are shown in table 1. The BE of the Li-doped tube, whether Li is inside or outside the nanotube, is position independent in most of the cases, or varies with the site occupied by the Li atom by about tens of meV in a few cases, which means that there is either no or quite a small diffusion potential barrier for the motion of the Li atom inside or outside the tubes.

The BE for a single Li inside is, in general, greater than that of the surface Li. For the (3, 3), (5, 0) and (4, 2) nanotubes, the BEs for a single inner (surface) Li atom are 0.92 (0.84), 2.58 (2.52) and 2.15 (1.93) eV, respectively. The Li concentration was increased by placing 2 Li atoms in the unit cell inside or outside the tubes. In the (3, 3) tube, we find that the BE

Table 1. The binding energy (BE) per Li atom in electronvolts for the various concentrations of encapsulation of Li atoms in (3, 3), (5, 0) and (4, 2) nanotubes. The averaged diameters of the tubes and the Li–C distances in ångströms are also included.

	(3, 3)			(5, 0)			(4, 2)		
Position of Li atoms	BE	Tube Diameter	Li–C distance	BE	Tube Diameter	Li–C distance	BE	Tube Diameter	Li–C distance
Inside 1-Li	0.92	4.35		2.58	4.16	2.20	2.15	4.31	2.19
(in-plane or			2.19						
between planes)			2.26						
Inside 2-Li	Unstable			1.59	4.20	2.13	2.15	4.32	2.19
Inside 5 Li	Unstable			Unstable			1.34	4.36	2.20
Surface 1-Li	0.84			2.52	4.13	2.15	1.93	4.30	2.30
mid-hexagon		4.58							
mid-bond		4.43	2.07						
Surface 2-Li	0.85	4.40	2.21	2.30	4.16	2.08	1.88	4.35	2.32
Surface 3-Li	Unstable			1.73	4.17	2.09			
Surface 4-Li	Unstable			1.34	4.19	2.27			
Surface 5-Li	Unstable			1.69	4.22	2.10			
Surface 6-Li	Unstable			1.48	4.24	2.00	1.74	4.30	2.20
Surface 8-Li	Unstable			1.59	4.21	2.11			
(Li in a plane)									
Surface 16-Li	Unstable			1.37	4.18	2.15			
(Li in two planes)									
Surface 18-Li	Unstable			Unstable			1.73	4.36	2.16
(Li in three planes)									
Surface 12-Li	Unstable			1.24	4.23	2.12	1.3	4.30	2.18
(Li in a plane)									

for 2 Li atoms drops to a negative value, meaning thereby no binding. On the other hand, for two Li atoms lying on the surface of the (3, 3) tube, the BE remains quite similar to that for one surface Li atom. For three surface Li atoms on the (3, 3) tube, the BE is calculated to be negative.

The results for the BEs for the Li-doped (5, 0) tube are quite different. Now two Li atoms are allowed inside the (5, 0) nanotube although the BE drops by about 40%. The Li–Li separation within the tube is 2.11 Å . The BE for two surface Li atoms decreases by about 9% as compared to one surface Li atom. For 8 or 12 surface Li atoms lying in one single plane in the unit cell, the BEs are 1.59 and 1.24 eV, respectively, whereas for 16 Li atoms lying in two different planes separated by 2.11 Å along the tube axis, the BE reduces to 1.37 eV. The BE decreases quickly with the number of surface Li atoms and also fluctuates.

We have also checked the calculation for 10 Li atoms lying in one plane in a unit cell and find a positive BE of about 1.30 eV. For 20 Li atoms lying on two planes separated by 2.11 Å on the tube axis, the BE is expected to be positive of the above order.

For the (4, 2) nanotube, the BEs for 1-Li or 2-Li atoms (having a large separation between them) encapsulated inside the tube on the tube axis are the same, 2.15 eV. For the maximum number of allowed 5 Li atoms placed inside on the tube axis with a Li–Li separation of 2.26 Å, the BE drops to 1.34 eV, showing the occurrence of screened repulsive Coulombian Li–Li interactions. We have increased the Li concentration by distributing 12 Li atoms on the tube surface in one plane normal to the tube axis, and obtain a BE of 1.3 eV. Alternatively, when 18 Li atoms were distributed among three different planes separated along the tube axis in the

unit cell, each plane containing 6 Li atoms, the BE turns out to be 1.73 eV. For the surface Li atoms again, the BE decreases with the number of absorbed Li atoms.

In table 1, the averaged tube diameters and the minimum Li–C distances have also been included. One does not see any obvious correlation between the BE and either the tube diameter or the Li–C bond length. However, in most of the cases, the BE decreases with increase in the Li–C separation.

Our results for the stability of the Li-doped nanotubes are in sharp disagreement with those of Liu and Chan (2003). Our values are higher than theirs. These authors (the sign of BE is opposite to ours) have found the Li-doped (3, 3) tubes unstable in contrast to our finding that the tubes are stable. Liu and Chan have determined BE over the bulk Li whereas we have obtained the values over the isolated Li atom. We have checked our BEs over the bulk Li, i.e., we calculated the energy of an Li atom in the bulk bcc solid, which is seen to be 0.52 eV lower than that of the isolated Li atom. For one Li atom encapsulated inside the tube, the present values of BE with respect to one bulk Li atom are 0.40, 2.05 and 1.63 eV for the (3, 3), (5, 0) and (4, 2) nanotubes, respectively, as compared to the values -0.48, 0.75 and 0.42 eV of Liu and Chan (as read from their paper). Our values are thus in sharp disagreement with those of Liu and Chan. One of the causes of this discrepancy may be their choice of a low value for the cut-off energy for the plane waves equal to 21.08 Ryd, in contrast to the present value of 60 Ryd. In our earlier discussion we found that the BEs remain invariant for a cut-off energy greater than 20 Ryd for the (3, 3) and (5, 0) tubes. However, for the case of (4, 2) nanotubes, the BEs for a cut-off energy of 20 Ryd are quite smaller than those for the cut-off energy of 60 Ryd. The BEs are also unreliable. For example, the BEs for one and two Li atoms inside the tube are 1.26 and 1.76 eV, respectively, for a cut-off energy of 20 eV, as compared to the same value of 2.15 eV for a cut-off energy of 60 Ryd. Thus the BEs of Liu and Chang for the (4, 2) tube are not converged values. In fact, the BEs for the Li-doped tubes stabilize at a cut-off energy of 60 Ryd only. However, this rules out this cause of discrepancy seen for the (3, 3) and (5, 0) tubes. Another cause of the discrepancy may lie in the choice of the pseudopotential which we have seen to affect the values of BEs. Liu and Chan have not mentioned the source of the pseudopotential used by them.

Our positive values of BEs with respect to the bulk Li atom obtained for all the Li nanotube configurations mean that the free Li atoms would prefer to be attached to the nanotubes instead of forming their own solid phase.

We will see later that there is nearly total transfer of charge from the inner or surface Li atoms to the nanotube, and the Li^+ ion has practically unit positive charge. The presence of another Li^+ ion in the vicinity of the first Li^+ will be unfavourable because of the strong repulsive Coulombian energy. However, the screening produced by the nanotube will reduce this strong repulsive energy significantly. The repulsive Coulombian energy is more than compensated by the attractive interaction between the Li^+ and the negatively charged nanotube for stable atomic configurations presented in this paper.

We find that the tubes are now buckled, i.e., they reveal a radial deformation. This deformation for (5, 0) and the (4, 2) tubes containing Li inside is quite small ($\sim$1–2%), but for all other cases in all the tubes, it is as high as 6–10%.

The Li–Li separations between the adjacent unit cells in the linear chains formed inside (outside) the (3, 3), (5, 0) and (4, 2) nanotubes containing one Li atom in the unit cell are seen to be 2.41 (2.41), 4.23 (4.24) and 11.29 (11.29) Å, respectively. The effects of Li–Li interaction and the Li–tube interactions will be visible in the physical properties of the nanotubes. The inclusion of one more Li atom in the unit cells of the (5, 0) and (4, 2) nanotubes (two Li atoms per unit cell) decreases drastically the Li–Li separation inside the tubes to 2.11 and 3.86 Å, respectively. Further

Table 2. The electronic density of states in the units of states/eV/unitcell for the various concentrations of Li atoms encapsulated in the (3, 3), (5, 0) and (4, 2) nanotubes.

Position of Li atoms	(3, 3)	(5, 0)	(4, 2)
Pristine	0.31	3.50	0.00
Inside 1-Li	2.31	1.50	0.77
(in-plane or between planes)			
Inside 2-Li	Unstable	0.53	4.15
Surface 1-Li			
(mid-hexagon)	2.4	1.36	0.80
(mid-bond)	4.0	1.40	
Surface 2-Li	3.28	1.40	5.27
Surface 3-Li	Unstable	3.20	
Surface 4-Li	Unstable	3.90	
Surface 5-Li	Unstable	1.47	
Surface 6-Li	Unstable	4.17	13.52
Surface 18-Li	Unstable		19.35

inclusion of one more Li atom to increase the Li concentration inside the (3, 3) or (5, 0) tube is not favoured. Thus, the saturated value of Li concentration inside the (3, 3) tube corresponds to the unit cell $C_{12}Li$, which means a maximum Li concentration of 8.3%. For the (5, 0) tube, the saturation concentration for the inside Li atoms corresponds to $C_{20}Li_2$, which is equivalent to an Li concentration of 10%. In the (4, 2) nanotube, the saturation concentration of the inner Li atoms corresponds to $C_{56}Li_5$, which means a concentration of 9%.

Turning towards the binding of surface Li atoms on the tubes, the saturation Li concentration for the (3, 3) tube for the stable $C_{12}Li_2$ configuration is 16.7%. On the other hand, for the (5, 0) tubes, 10 surface Li atoms lying in one plane are energetically allowed. As one unit cell can accommodate two planes of Li atoms separated by a distance of 2.11 Å along the tube axis, the saturation Li concentration corresponds to the unit cell $C_{20}Li_{20}$ which means a 100% absorption of Li atoms.

Similarly, for the (4, 2) nanotube, we have seen that 12 Li atoms on the surface of the tube lying in one single plane are stable. The (4, 2) tube can accommodate five planes of Li atoms situated along the tube axis in the unit cell and thus a unit cell $C_{56}Li_{60}$ is also stable, which means a saturation concentration of more than 100%.

For the saturation absorption of Li atoms on the (5, 0) and (4, 2) tubes, one observes a cylindrical tube of Li^+ ions enclosing the tube similar to metal nanoring.

3.2. Electronic structure

The computed self-consistent electronic charges within an atomic Li diameter of 1.3 Å for the various Li and nanotube configurations reveal that in all the configurations of Li inside or outside the tubes, the charge is the same and is about 3–4% of e. This means transfer of most of the electronic charge of the s orbital of Li to the nanotube. The DOS has been calculated for 51, 26 and 16 k-points in the BZ for the (3, 3), (5, 0) and (4, 2) tubes, respectively, with a broadening of 0.055 eV and is presented in table 2. The Fermi level (E_F) has been chosen as the origin of energy. For the DOS, the full units are states/eV/unitcell and for brevity in our further discussion we will write units instead of the full units.

Li-doped (3, 3) nanotubes. The electronic structure and the DOS for the pristine (3, 3) nanotubes are presented in figure 2(a). The bonding and the anti-bonding (24, 25) states cross

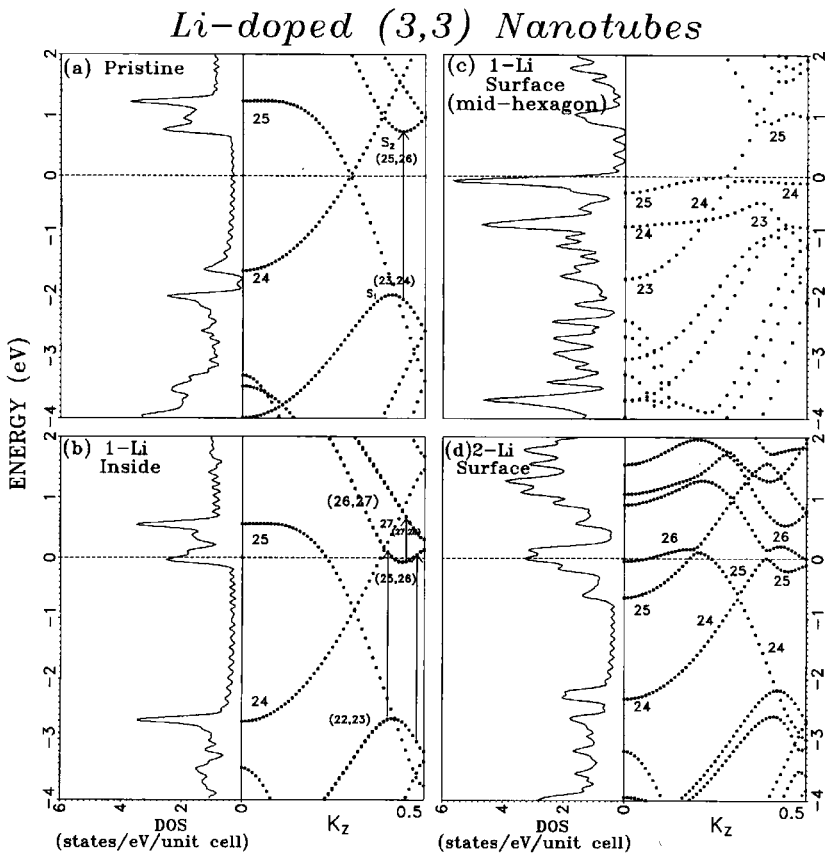

Figure 2. The electronic structure and the density of electron states in the vicinity of the Fermi level for (3, 3) nanotubes: (a) pristine, (b) 1-Li inside, (c) 1-Li on the surface, and (d) 2-Li on the surface. The doubly-degenerate topmost filled and the lowest unfilled states have been marked as (23, 24) and (25, 26) near the BZ boundary for the pristine tube. The numbering is different for each system at various values of k_z. Some typical optical transitions have also been demonstrated.

at E_F, and the tube is metallic as expected by symmetry consideration. The DOS at E_F is 0.31 units. In figure 2(a), we have shown the highest occupied single 24th state and the lowest unoccupied single 25th state before the crossing point $k_z = 0.3$. Above the crossing point for $k_z > 0.4$, we also depict the doubly-degenerate occupied (23, 24) states and the doubly-degenerate unoccupied (25, 26) states which have come up (down) in the valence (conduction) band region. These states contain two saddle points S_1 and S_2 near the boundary of the BZ in the vicinity of E_F. In fact these states are seen to contribute to the optical transition.

1-Li. The electronic structure and the DOS for 1-Li-doped nanotubes both inside and outside the (3, 3) nanotubes are presented in figures 2(b) and (c), respectively. For Li inside the tube, E_F is shifted upwards by the electron donated by Li and it approaches a vHs present in the conduction band region at the centre of the BZ. As pointed out earlier, the inclusion of an Li atom on the tube axis does not affect the symmetry of the tube, and therefore the overall electronic structure is retained. At E_F, the bonding and anti-bonding states are now the hybridized C(p)–Li(p) states. The shifting increases the DOS of the doped tube to a peaked

value of 2.31 units. The results for 1-Li inside the (3, 3) tube are in overall good agreement with those of Liu and Chan (2003) except for the magnitudes of the DOS.

On the other hand, the electronic structure for the Li-atom residing on the surface of the (3, 3) tube is drastically changed in the neighbourhood of E_F. This is the consequence of the breaking of the symmetry of the host tube by the Li atom residing on the surface. The bonding–antibonding carbon states no more cross but split with a minimum energy separation of about 0.9 eV. The upper state is a quit flat hybridized C-(p)–Li(p) orbitals state having quite appreciable contribution from the Li (p) orbitals. The band encompassing E_F is quite narrow, enhancing the DOS to about 2.4 (4.0) units for an Li atom residing at the mid-hexagonal (-bond) site on the surface of the tube.

2-Li. The electronic structure and the DOS for the diametrically placed two surface Li atoms on the (3, 3) nanotube shows quite a different behaviour (figure 2(d)). A state from the conduction energy region descends below E_F and mixes with the flat band already present in the 1-Li-doped tube. The states split near E_F. The vHs touches E_F, leading to a quite high value of 3.28 units for the DOS.

Li-doped (5, 0) nanotubes. The pristine (5, 0) tube is expected to be semiconducting by symmetry considerations. However, because of the strong curvature effects, a state 'α' lying in the conduction band region next to E_F descends quite appreciably and makes the nanotube conducting (figure 3(a)). A vHs from the valence band region occurs very near to E_F and enhances the DOS to 3.5 units. The next conduction state lies about 0.5 eV higher at $k_z = 0$.

1-Li. The electronic structure and DOS for 1-Li-doped (5, 0) nanotubes for both Li inside and outside doping are presented in figures 3(b) and (c), respectively. For both types of doping, most of the electron charge of Li is transferred to the nanotube, and it fills the states lying at E_F, resulting in a small shift of E_F upwards. As pointed out earlier, the inclusion of an Li atom on the tube axis does not affect the symmetry of the tube, and therefore the overall electronic structure is retained. In fact, the second conduction band crosses the $k_z = 0$ point slightly below E_F, and reduces the DOS at E_F. Far from E_F, the states at the BZ boundary split.

For Li residing on the surface, the states split further at the $k_z = 0$ point also. This is the consequence of the breaking of the symmetry of the host tube by the Li atom residing on the surface. There is a drastic alteration in the electronic structure of the Li-doped tube. The DOS at E_F is similar for both types of doping, and is about 1.4–1.5 units.

2-Li. The electronic structure and the DOS are shown in figure 3(d). More transferred charge from Li atoms fills the second conduction state and as the vHs is far from E_F, the DOS for the Li inside (outside) drops to 0.61 (1.4) units. The states at the $k_z = 0$ point and at the BZ boundary split for the encapsulated 2-Li atoms inside and this splitting is further enhanced in terms of the number of states for the 2-Li ions on the surface of the (5, 0) nanotube. It is noted that a vHs named here as 'β' causing a quite high DOS appears at about 1.6 eV.

3-Li. The electronic structure and DOS for 3-Li surface atoms are depicted in figure 4(a). Four conduction bands now descend below E_F at $k_z = 0$. An interesting feature is that a vHs occurs at E_F which enhances the DOS appreciably to 3.2 units. The vHs 'β' causing a quite high DOS appears above at about 1.2 eV.

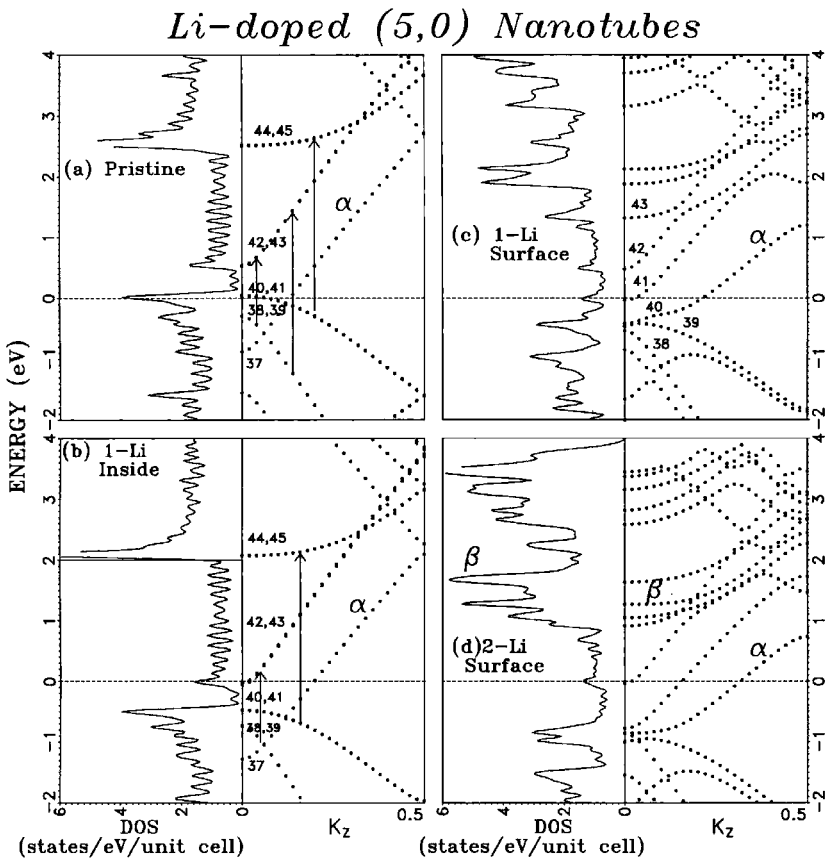

Figure 3. The electronic structure and the density of electron states in the vicinity of the Fermi level for (5, 0) nanotubes: (a) pristine, (b) 1-Li inside, (c) 1-Li on the surface, and (d) 2-Li on the surface. The doubly-degenerate topmost filled and the lowest unfilled states have been marked as (38–41) and (42–45) near the centre of the BZ for the pristine tube. The numbering is different for each system at various values of k_z. Some typical optical transitions have also been demonstrated.

4-Li. For 4-Li ions residing on the surface of the nanotube, the band structure and the DOS are presented in figure 4(b). Five conduction bands descend below E_F at $k_z = 0$. Again, one vHs occurs at E_F and the DOS is increased to 3.9 units. The vHs 'β' descends further and appears at about 0.6 eV.

5-Li. The electronic structure and the DOS for five surface atoms per unit cell are presented in figure 4(c). The conduction bands descend more and the separation between the pairs of the bands is reduced. The fifth conduction band is now a bit above E_F at the $k_z = 0$ point. One vHs occurs just above E_F and the DOS decreases to 1.47 units. The vHs 'β' descends further and appears at about 0.4 eV.

6-Li. The electronic structure and the DOS for six surface atoms per unit cell are presented in figure 4(d). Again, now five conduction bands descend below E_F at the $k_z - = 0$ point. One vHs occurs very close to E_F and the DOS is increased to a maximum value of 4.17 units.

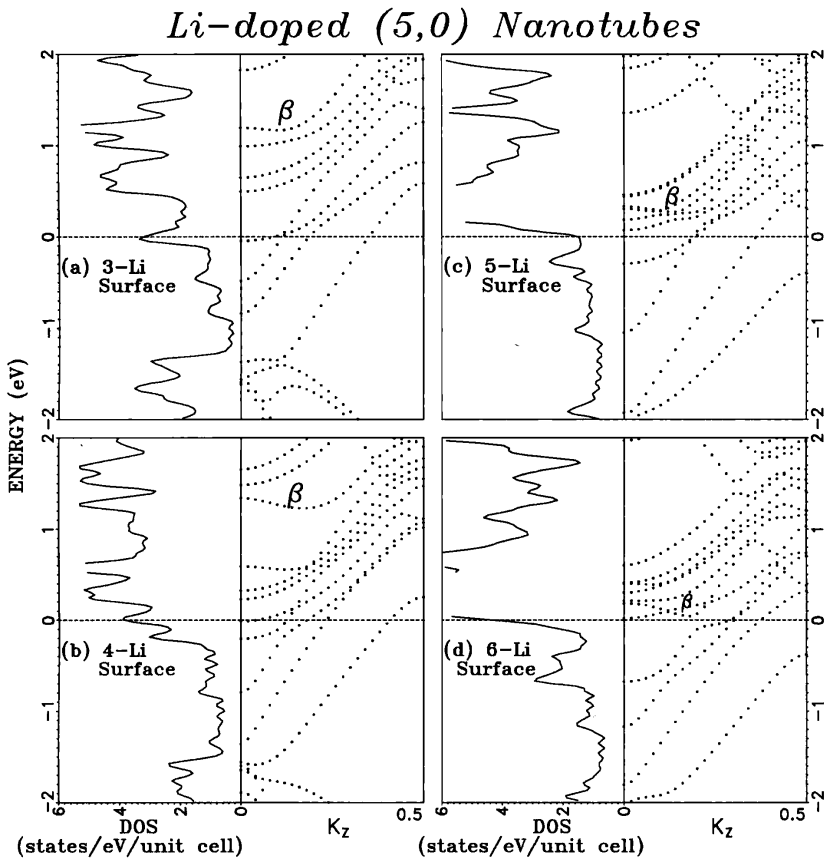

Figure 4. The electronic structure and the density of electron states in the vicinity of the Fermi level for (5, 0) nanotubes: (a) 3-Li on the surface, (b) 4-Li on the surface, (c) 5-Li on the surface, and (d) 6-Li on the surface.

The vHs 'β' descends and appears at about 0.2 eV. It seems that the further addition of one or two Li atoms to the (5, 0) tube will shift the 'β' vHs to match it with E_{F}. This will lead to a very high value of the DOS at E_{F}.

In (5, 0) nanotubes doped with 1-, 2-, and 5-Li surface atoms, the DOS decreases but regains its pristine DOS value for the 3-, 4-, and 6-Li surface atoms. The highly Li-doped (5, 0) tube may be a candidate not only for very high conductivity but also even superconductivity.

Li-doped (4, 2) nanotubes. The pristine (4, 2) nanotube is semiconducting and its electronic structure and DOS are shown in figure 5(a).

1-Li. The electronic structure and DOS for 1-Li-doped (4, 2) nanotube are presented in figures 5(b) and (c). The incorporation of an Li atom inside or outside the (4, 2) nanotube shifts E_{F} by different magnitudes upwards, making the tube metallic. As the tube has no obvious symmetry, the inclusion of Li atom on the tube axis or on the surface does not affect the overall electronic structure. The DOS for 1-Li atom incorporated inside (outside) the tube becomes 0.77 (0.80) units.

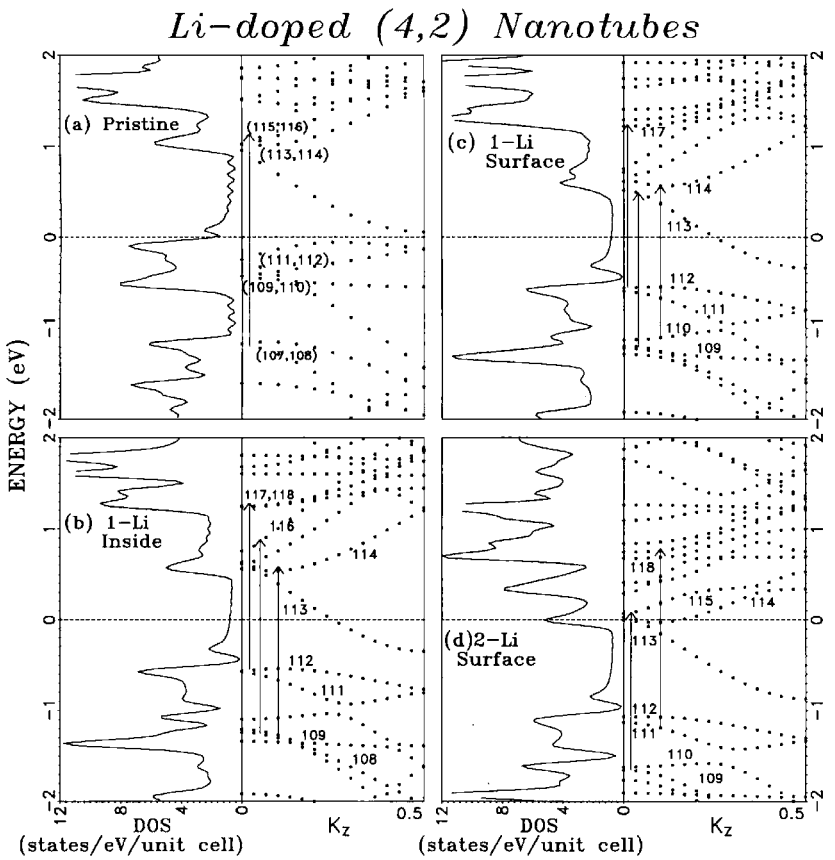

Figure 5. The electronic structure and the density of electron states in the vicinity of the Fermi level for (4, 2) nanotubes: (a) pristine, (b) 1-Li inside, (c) 1-Li on the surface, and (d) 2-Li on the surface. The doubly-degenerate topmost filled and the lowest unfilled states have been marked as (107–112) and (113–116) near the centre of the BZ for the pristine tube. The numbering is different for each system at various values of k_z. Some typical optical transitions have also been demonstrated.

2-Li. For a 2-Li doped (4, 2) tube, E_F further shifts up and touches a vHs lying in the conduction band region (figure 5(d)). The DOS for the 2-Li atoms inside the tube thus jumps to 4.15 units, and for 2-Li atoms absorbed on the surface, the DOS is enhanced to 5.27 units.

For a larger number of surface Li atoms on the (4, 2) tube, i.e., 6 and 18 Li atoms, although the DOS is enhanced to 13.52 and 19.35 units the DOS per C atom is small (see table 2).

3.3. Optical absorption

We calculate the optical absorption spectra of the isolated nanotube and the Li-doped tubes by using the absorption coefficient (Hybertson and Needles 1993) as

$$\alpha(\omega) = \frac{4\pi^2 e^2}{ncm^2\omega V_c} \sum_{v,c,\vec{k}} |\vec{\varepsilon} \cdot \vec{p}_{cv}(\vec{k})|^2 \delta(E_c - E_v - \hbar\omega), \tag{1}$$

with m and e as the electron mass and charge, c as the velocity of light, n the refractive index, and V_c the unit cell volume including the empty space; $\vec{\varepsilon}$ denotes a unit electric vector of the

Table 3. The RBM frequencies in cm^{-1} for the various types of encapsulation of Li atoms in (3, 3), (5, 0) and (4, 2) nanotubes.

Position of Li atoms	(3, 3)	(5, 0)	(4, 2)
Pristine	532	526	527
Inside 1-Li	546 (unrelaxed)	503	519
	490 (between planes)		
	495 (in-plane)		
Inside 2-Li	Unstable		515
Inside 5-Li	Unstable		502
Surface 1-Li	442 (mid-hexagon)		
	445 (mid-bond)	505	518
Surface 2-Li	544	502	507
Surface 3-Li	Unstable	489	
Surface 4-Li	Unstable		
Surface 5-Li	Unstable	476	

incident polarized light. E_c and E_v are the energies of the conduction and the valence states for the wavevector **k**. The momentum operator matrix element $\vec{p}_{cv}(k)$ is given by

$$\vec{p}_{cv}(\vec{k}) = \langle \psi_c, \vec{k} | \vec{p} | \psi_v, \vec{k} \rangle, \tag{2}$$

where Ψ_c and Ψ_v denote the wavefunctions of the conduction and the valence states, respectively. $\vec{p}$ is the momentum operator.

In the actual calculation, for simplicity, we consider the polarization of light confined in one direction x, y or z. Further, the absorption has been obtained using a broadening of 0.1 eV to avoid the spiky structure arising from our choice of a coarse grid in the BZ to cope with the limited memories of computer available to us.

The no-phonon optical absorption for the incident electromagnet polarization along the tube axis and normal to it obtained for the various Li tube configurations are compared with the pristine tubes in figures 5–8. In all cases, the absorption normal to the axis of each nanotube is quite small.

(3, 3) nanotubes. For the pristine (3, 3) nanotube, the optical absorption along the tube axis is shown in figure 6(a). One observes a strong peak having its low-energy edge at 2.9 eV along with weak absorption around 3.5 eV. These peaks are quite close to the experimentally observed peak at 3.1 eV by Lie *et al* (2001) and Liang *et al* (2002) in 4 Å nanotubes. The present value of 2.9 eV is also near to the calculated values of Machon *et al* (2002) and Liu and Chan (2003) who have obtained a peak at 2.8 eV.

The transition between the states numbered as 24th and 25th at $k_z = 0$ are forbidden by symmetry considerations. It should be noted that appreciable optical absorption for (3, 3) nanotubes whether pristine or doped with Li atoms is observed only for the wavevector range of $k_z = 0.38$–0.50. Also, the main peak at 2.9 eV arises from the transitions between the doubly-degenerate occupied (23, 24)th and the unoccupied (25, 26)th states in the wavevector range of $k_z = 0.4$–0.48, as shown in figure 2(a). In fact, the saddle points S_1 and S_2 shown earlier in figure 2(a) occurring in these states are responsible for intense transitions. The other peaks involve the transition between the filled (23, 24) states and the vacant (25–27) states in the above wavevector range. It may be cautioned that the present numbering of states is different at different values of $k_z > 0.40$ and is totally different from the numbering of states at $k_z = 0$.

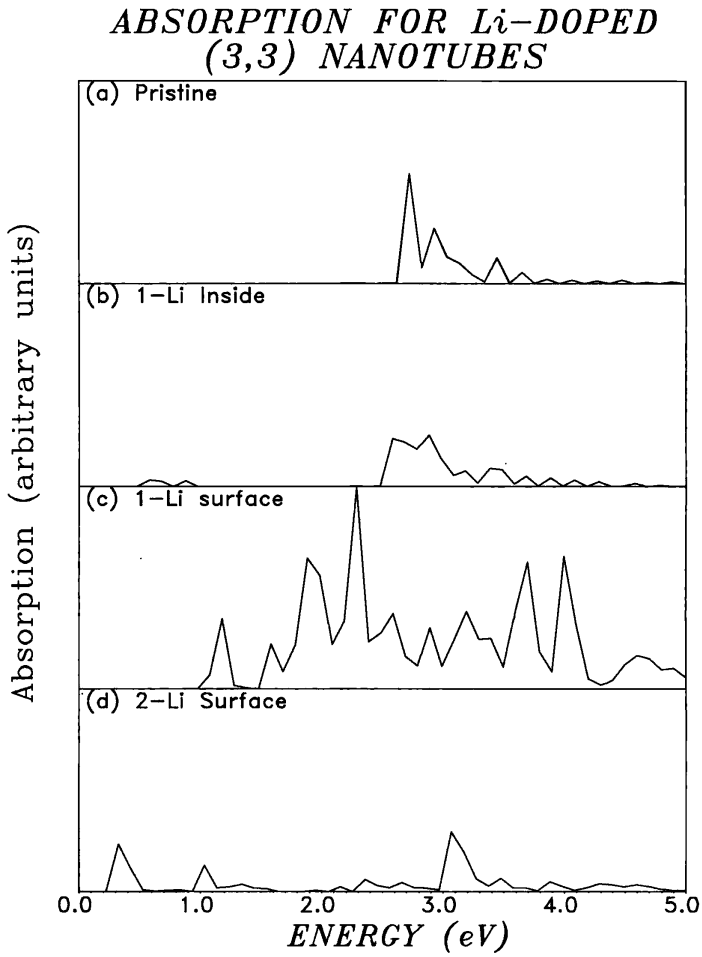

Figure 6. Absorption spectra in the energy region 0–5.0 eV for (3, 3) nanotubes: (a) pristine, (b) 1-Li inside, (c) 1-Li on the surface, and (d) 2-Li on the surface.

1-Li. For the (3, 3) nanotube doped with one Li per unit cell inside it, the peak structure (figure 6(b)) is quite similar to that of the undoped tube. It arises from the fact that the total valence charge of the Li atom which is transferred to the nanotube does not alter very significantly the electronic structure of the undoped nanotube but fills the topmost states and shifts E_F upwards.

For the Li-doped (3, 3) tube too, as regards to the participation of the states giving rise to absorption, the situation is exactly similar to that of the pristine tube. However, there are differences. A peak similar to the pristine tube occurs at 2.9 eV but it contains a dip. The state containing the saddle point S_2 has descended, and in a small wavevector range it has crossed the E_F. The strong absorption in the energy region 2.9 eV arises from the transitions between the filled doubly-degenerate (22, 23) states and the vacant doubly-degenerate states (25, 26), as shown in figure 2(b). In the wavevector range where the conduction states (25, 26) are below E_F and are now filled, they show weak optical absorption by sending the electron to the next vacant states (27, 28) in the energy range of 0.5–0.9 eV. As these transitions no more contribute to peak at 2.9 eV, a dip appears.

For the Li atoms absorbed on the surface of the (3, 3) nanotube at the mid-hexagonal site, the optical absorption as shown in figure 6(c) is very strong and quite different. It possesses a spiky structure. The absorption now extends up to the low-energy region (up to 1.0 eV) because of the participation of all the filled and the unfilled states existing in the vicinity of E_F, as shown in figure 2(c). There is a large dipole moment between the Li^+ ion and a few negatively charged C atoms of the nanotube and this gives rise to quite high values for the matrix elements. Several extra strong peaks appear at 1.8, 2.2, 3.6 and 4.0 eV. The optical transitions now involve the filled (18–24) states and the vacant (25–29) states. It is not possible to show this very large number of transitions in figure 2(c). The absorption for the two different sites of Li-ion on the tube surface, i.e., mid-hexagon and -bond, are also different in the low-energy region.

For two surface Li ions as shown in figure 6(d), the overall absorption is quite weak and it shifts to the low-energy side. Peaks appear at 0.4, 1.0, and 3.0 eV. Similar to the 1-Li surface case, a large number of the occupied and the unoccupied states lying in the vicinity of E_F participate in the optical transitions. The main peaks at 0.4 and 1.0 eV originate from the transitions between the filled 25th state and the vacant 26th and 28th states, respectively. The peak at 3.0 eV arises from the participation of the filled 22nd state and the vacant 27th state.

(5, 0) nanotubes. The optical absorption for the pristine (5, 0) nanotube shown in figure 7(a) reveals two broad peaks centred at 0.9 and 2.5 eV. The present peaks are quite near to the experimental peaks observed at 1.2, 2.1 and 3.1 eV for 4 Å carbon tubes by Lie *et al* (2001) and Liang *et al* (2002). Also, the present peaks are quite close to the calculated values of 1.2 and 2.3–2.4 eV in Machon *et al* (2002), Liu and Chan (2003). It may be mentioned that the optical absorption arises from the wavevector range of $k_z = 0$–0.24 and involves all the 37th to 45th states at different values of k_z. The peak around 0.8 eV arises from the transitions between the doubly-degenerate occupied (38, 39) states and the doubly-degenerate unoccupied (42, 43) states. On the other hand, the peak at 2.5 eV originates from the transitions between the (40, 41) and the (44, 45) states. The transitions between the occupied (40, 41) and the unoccupied (42, 43) states are forbidden by symmetry considerations similar to the (3, 3) tube.

1-Li. For 1-Li doped inside the (5, 0) nanotube, the absorption presented in figure 7(b) now reveals peaks at 0.8 and 2.6 eV. A split weak peak appears at 1.0 eV. The participation of the states in the absorption is exactly similar to that seen earlier in the pristine (5, 0) tube except for the shifting and the splitting of some peaks. It may be noted that the optical absorption for the pristine or the Li-doped (5, 0) tube arises mainly from the wavevector range of $k_z = 0$–0.08. Weak absorption above 3.0 eV is seen for the wavevector range of $k_z = 0.12$–0.24.

For one Li atom residing on the surface of the tube, there is no enhanced dipole moment between the Li^+ ion and the negatively charged nanotube because of the distribution of negative charge on a larger number of C atoms. However, the electronic structure is drastically changed because of the loss of host tube symmetry. As shown in figure 7(c), several strong peaks appear at 0.4, 0.65, 0.85, 1.05 and 2.35 eV. The peaks at 0.35–0.45 eV originate from the transitions between the occupied (40, 41) states and the unoccupied 42th state, whereas the peak at 0.65–0.85 eV arises from the filled 38th state and the unoccupied 42th state at different values of k_z. The peak at 1.0 eV originates from the transitions between the occupied (37–41) states and the unoccupied (41–43) states. It should be kept in the mind that the state 41 is occupied below a small value of k_z but becomes an unoccupied state thereafter. The transitions between the filled (40, 41) states and the vacant 45th state give rise to peak at 2.35 eV.

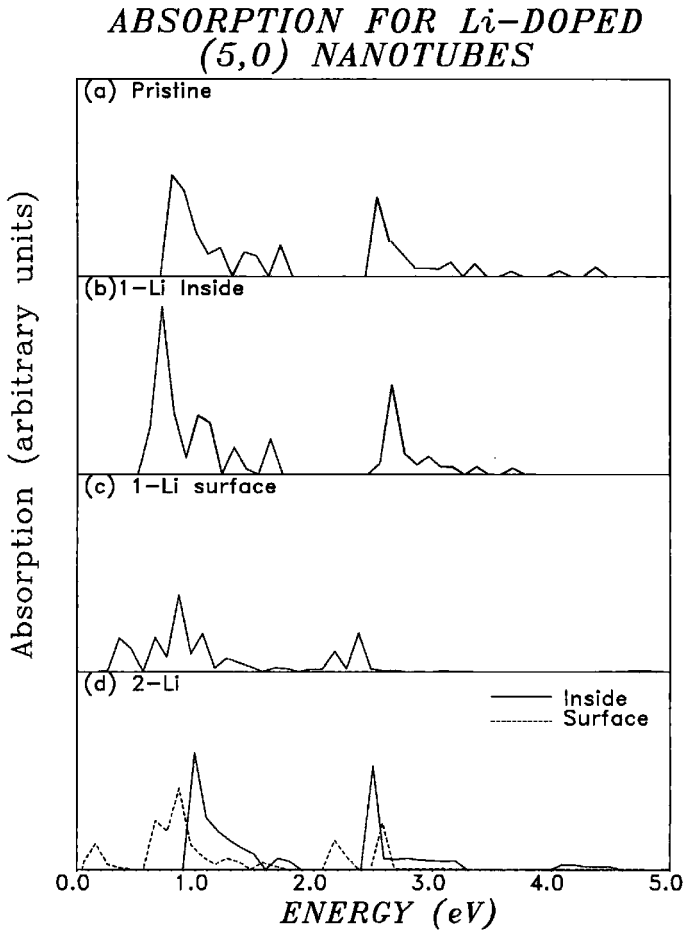

Figure 7. Absorption spectra in the energy region 0–5.0 eV for (5, 0) nanotubes: (a) pristine, (b) 1-Li inside, (c) 1-Li on the surface, and (d) 2-Li inside or on the surface.

2-Li. For the 2-Li atoms inside the (5, 0) tube as shown in figure 7(d), one observes one broad strong peak having a lower edge at the 1.0 eV peak, and a sharp peak centred at 2.5 eV. The lower peak arises from the transitions between the filled (37–39) states and the vacant (42, 43) states. The higher peak at 2.5 eV originates from the transitions between the occupied (40–41) states and the unoccupied (44, 45) states.

For the 2-Li atoms lying on the surface as shown in figure 7(d), there appear a strong peak centred at 0.9 eV and three weak peaks at 0.16, 2.17 and 2.58 eV. All the peaks, including the strong peak around 0.9 eV, originate from the transitions between the occupied (38–41) states and the unoccupied (42, 43) states.

3-Li. The optical absorption for 3-Li surface atoms as shown in figure 8(a) reveals a strong broad band having its low-energy edge at 0.78 eV and a weak broad peak centred at 2.6 eV. The low-energy peak arises from the transitions between the filled (39–41) states and the vacant (42, 43) states at various values of k_z. The high-energy peak originates from the transitions between the occupied (38–41) states and the unoccupied (42–46) states.

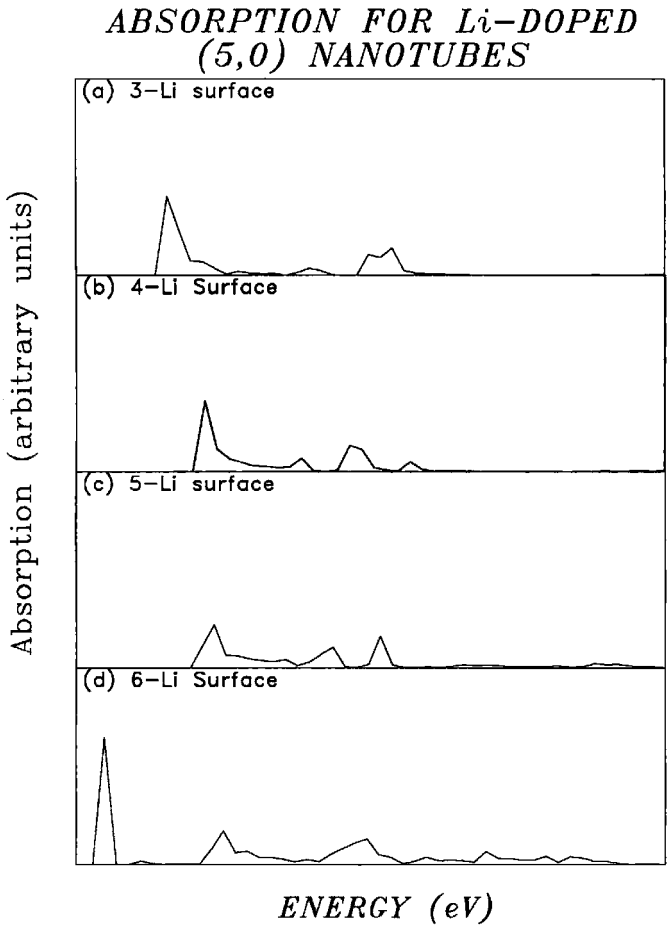

Figure 8. Absorption spectra in the energy region 0–5.0 eV for (5, 0) nanotubes: (a) 3-Li on the surface, (b) 4-Li on the surface, (c) 5-Li on the surface, and (d) 6-Li on the surface.

4-Li. The optical absorption for 4-Li surface atoms as shown in figure 8(b) shows a strong broad band having its low-energy edge at 1.1 eV and a weak peak centred at 2.4 eV. The low-energy peak at 1.1 eV arises from the transitions between the filled (39–41) states and the vacant 43th state at various values of k_z. The participation of the occupied (38–42) states and the unoccupied (44, 45) states gives rise to a broad peak at 2.4 eV.

5-Li. The optical absorption for 5-Li surface atoms as shown in figure 8(c) reveals a strong broad band having its low-energy edge at 1.1 eV and extended up to 2.6 eV. This absorption arises from the transitions between the filled (38–41) states and the vacant (44–50) states at various values of k_z. The high-energy peak originates from the transitions between the occupied (38–41) states and the unoccupied (42–46) states.

6-Li. For 6-Li surface atoms on the (5, 0) tube, in the absorption shown in figure 8(d), one observes a very strong peak at 0.24 eV and two weak peaks at 1.25 and 2.5 eV along with continuous absorption up to 5 eV. The peaks at 0.24 and 1.25 eV arise from the transitions

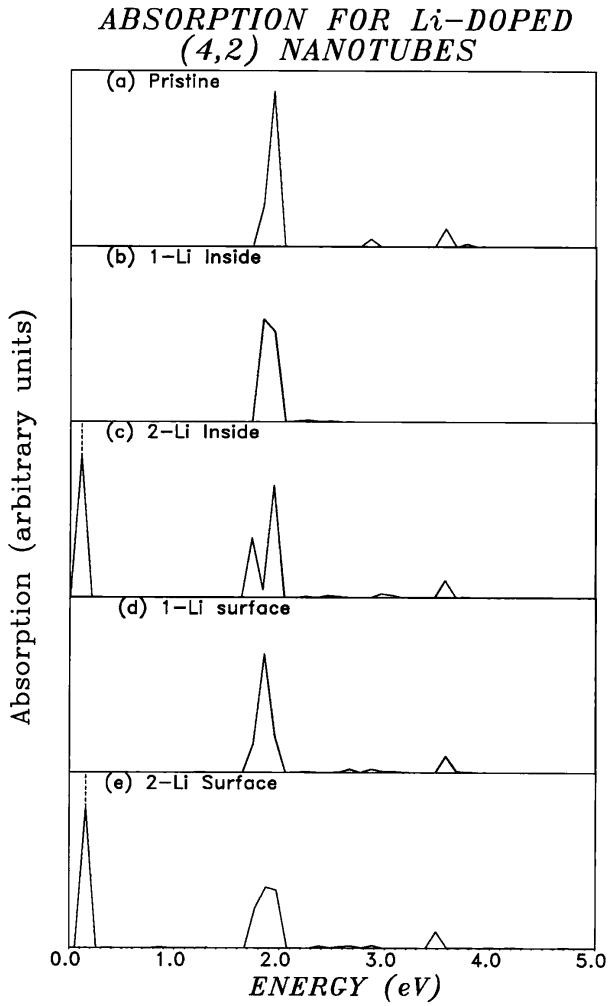

Figure 9. Absorption spectra in the energy region 0–5.0 eV for (4, 2) nanotubes: (a) pristine, (b) 1-Li inside, (c) 2-Li inside, (d) 1-Li on the surface and (e) 2-Li on the surface.

between the filled 43rd and 40th states and the common unfilled 44th state, respectively. The peak at 2.5 eV originates from the various combinations of the filled (38–41) states and the unoccupied (48–50) states.

(4, 2) nanotubes. For the (4, 2) nanotube configurations we have obtained the optical absorption for one k-point only, in order to have manageable computer time. For the pristine (4, 2) nanotube, the optical absorption is shown in figure 9(a). A very strong peak occurs at 1.95 eV along with two very weak peaks at 2.9 and 3.6 eV. The strong peak at 1.95 eV originates from the transitions between the occupied (107, 108, 111) states and the unoccupied (115, 116, 118) states at $k_z = 0.0$.

Our peaks are in good agreement with the measured peaks at 2.1 and 3.1 eV for 4 Å carbon tubes in Lie *et al* (2001) and Liang *et al* (2002) and the calculated peaks at 1.9, 2.9–3.0 and 3.6 eV in Machon *et al* (2002) and Liu and Chan (2003).

For the 1-Li doped inside the (4, 2) nanotube, as shown in figure 9(b), there appears a quite strong peak at 1.9 eV. This peak originates from the transitions between the various combinations of the occupied (108, 109, 111, 112) states and the unoccupied (114, 116, 117, 118) states.

For 1-Li atom on the (4, 2) tube surface, the absorption shown in figure 9(c) reveals a strong peak at 1.85 eV which originates from the transitions between the various combinations of the occupied (108–112) states and unoccupied (113, 114, 117, 118) states.

For 2-Li inside the (4, 2) tube, there appear a very strong peak at 0.1 eV and a weak peak at 1.9 eV. The strong peak arises from the transitions between the occupied 113th state and the vacant 116th state which are very close to each other. The weak peak at 1.9 eV originates from the filled (111, 112) states and the unoccupied (117, 118) states.

For the two surface Li atoms, the absorption reveals a very strong peak at 0.05 eV and a weak peak near 1.9 eV. The strong peak at 0.05 eV originates from the very closely spaced occupied 113th state and the unoccupied (114, 115) states. The peak at 1.9 eV arises from the transitions between the filled (111, 112) states and the vacant (118, 119) states.

3.4. Vibrational frequencies

It is known that the radial breathing A_{1g} mode is sensitive not to the nanotube structure but to the nanotube radius. After employing a frozen phonon approximation, we have calculated the frequency of the even parity A_{1g} radial breathing mode (RBM) for the isolated tube and the various ropes, which can be measured by Raman scattering. We study the variation of system energy with the very small displacements of atoms in the radial directions of the nanotubes, and evaluate the harmonic and cubic anharmonic force constants at the minimum system energy where the forces on the atoms vanish. The computed RBM frequencies for the pristine (3, 3), (5, 0), and (4, 2) tubes and for the Li-doped tubes along with their diameters are presented in table 3. For the pristine (3, 3), (5, 0), and (4, 2) nanotubes, the RBM frequencies are 532, 526 and 527 cm^{-1}. As the diameters of the three types of the tubes are 4.21, 4.09 and 4.29 Å, respectively, we find no correlation between the RBM frequencies and the diameters of the tubes. For the (5, 0) tube the diameter is the smallest one among all the tubes and so is the RBM frequency, in contrast to a behaviour expected from the inverse diameter law. The present values are quite close to a Raman peak at 534 cm^{-1} measured by Tang *et al* (1998) in single wall nanotubes having diameter smaller than 7 Å and to the measured peaks at 510, 550, 580 cm^{-1} in the pristine 4 Å nanotubes formed inside the microporous zeolite by Ye *et al* (2003). Liu and Chan (2003) have also obtained these values as 538, 525 and 529 cm^{-1}, quite near to ours, after employing a simple harmonic oscillator problem. We observe a strong anharmonicity in the radial breathing mode vibrations.

In the calculation of RBM frequency for Li-doped tubes, the Li atoms inside the tube remain at rest, but for Li atoms lying on the surface we assume that they move radially in phase with the carbon atoms of the tube. The vibrating mass in RBM is the total mass of the unit cell.

For the Li-doped nanotubes, the C atoms relax away from the axes, and the diameters of all the nanotubes are increased by 1 to 9% on account of the absorption of the Li atoms inside or outside. This dilation or widening of the tubes incurs a softening in the interatomic interactions and decreases the RBM frequencies, as is clear from table 3. For one Li atom residing inside the (3, 3) tube, the dilation of the diameter is 3%, and the RBM frequency for the different locations of Li drops from 532 cm^{-1} to approximately 493 ± 3 cm^{-1}. If the dilation is ignored, the frequency is enhanced to 546 cm^{-1}, supporting the expectation that the attractive Coulombian interactions between the positively charged Li^+ and the negatively charged C atoms of the tube will enhance the force constants. However, in practice, in the

relaxed geometries one finds that the effects of dilation mask the effects of this enhanced interaction. For one surface Li atom, the dilation is enhanced to 5–9%, reducing the RBM frequency to approximately 443 cm^{-1}. However, in contrast, for two Li atoms on the surface of the (3, 3) tube, in spite of dilation of a similar magnitude, the RBM frequency is enhanced to 544 cm^{-1}, an increase of 12 cm^{-1}.

For the (5, 0) nanotubes, the dilation is about 3–4% for all the doped tubes containing Li atoms inside or outside it, irrespective of the number of absorbed Li atoms. The RBM frequency drops from 526 to 476 cm^{-1}.

For the (4, 2) nanotubes, the optimized diameters of the Li are dilated within 2% and this reduces the RBM frequency from 527 to 502 cm^{-1}.

On making comparison of the present results with the experimentally observed RBM frequencies in the pristine 4 Å tubes with different chiralities doped with the various concentrations of the Li-atoms obtained by Ye *et al* (2003), we find some discrepancies. The present values of 532, 526 and 527 cm^{-1} obtained for the pristine tubes are close to the experimental frequencies, 510, 550 and 580 cm^{-1}. The discrepancies are of the order of 3% for the lower frequencies and 9% for the higher frequency. It should be noted that similar discrepancies will appear for the RBM frequencies as calculated by other authors (Liu and Chan 2003).

In the Raman data available for the Li-doped tubes inside zeolites the experimental frequencies at 510 and 580 cm^{-1} are seen to be unaffected by the Li doping, whereas the frequency at 550 cm^{-1} shifts to 568 cm^{-1} in the saturated Li-doped sample. Our study reveals that, in general, the RBM frequency decreases with the doping of one or more Li atoms for all the 4 Å tubes because of the dilation of the diameters of the tubes. The only exception is the (3, 3) nanotube doped with two surface Li atoms. In the absence of dilation the RBM frequency increases with Li doping as expected, with enhanced force constants.

4. Conclusions

The incorporation of Li atoms on all types of 4 Å nanotubes dilates the tube diameters. The minimum Li–C distances also vary. The binding of Li inside the tube is, in general, stronger than that for the tube containing Li atoms on the surface. The BE decreases with the number of doped Li atoms for $n > 2$. The saturation Li concentration inside each Li-doped tube lies in a range of 8–10%. On the other hand, the saturation concentration of Li atoms adsorbed on the tube surfaces of the achiral (5, 0) and (4, 2) tubes is as high as 100%. Our BEs are higher than those reported by earlier workers.

The electronic structure of the pristine tube remains practically unchanged (except for the upward shifting of E_F) by the Li atoms inside the tube on the axis as a consequence of the preservation of the point-group symmetry by doping. In contrast, surface Li atoms, in general, destroy the symmetry of the host lattice (except for the (4, 2) tube, which has practically no symmetry) and drastically alters the electronic structure.

In general, Li doping increases the DOS except for the (5, 0) tube. On doping with one Li atom inside (outside) the tube, the DOS in the doped (3, 3) nanotube increases by 8 (8 and 13) times, whereas in the doped (5, 0) tubes, it decreases by more than 60%. The Li doping makes the semiconducting (4, 2) nanotube metallic. The doping of the (4, 2) tube with two Li atoms inside the tube enhances the DOS to 4.15 units.

The absorption of two Li atoms on the surface of the (3, 3) tube increases the DOS by about 10 times that of the pristine tube, i.e., to 3.28 units, whereas for a similar surface doping of the (5, 0) tube, the DOS is small and is quite near that for one surface Li. For the (4, 2) tube, the DOS further increases to 5.27 units.

For the (5, 0) tube, the encapsulation of two Li atoms per unit cell inside the tube decreases further the DOS to a value of 0.53 units. For more than two Li atoms up to six Li on the surface of the (5, 0) tube, the DOS fluctuates between 1.40 and 4.17 units (a value for six Li atoms per unit cell).

For a larger number of surface Li atoms on the (4, 2) tube, i.e., 6 and 18 Li atoms, although the DOS is enhanced to 13.52 and 19.35 units the DOS per C atom decreases.

For one inside Li atom in every tube, the peak structure in the optical absorption remains the same as that of the pristine tube. For Li atoms absorbed on each type of tube surface, different types of structures are observed, extending to the low-energy region in some cases.

The optical absorption is enhanced by one surface Li atom doping in the (3, 3) nanotube because of the occurrence of a large dipole moment between the Li^+ ion and the negatively charged nanotube. However, this effect is not visible in other types of tubes where the electronic charge donated by the Li atom is distributed on a comparatively large number of atoms in the unit cell and reduces the amount of negative charge on C atoms of the tube and the resulting dipole moment.

For two Li atoms encapsulated inside the (4, 2) nanotube there is an occurrence of strong absorption near 0.1 eV, and the peak at 2.0 eV also splits. For Li atoms absorbed on the surface of the (4, 2) tube, in all cases a peak similar to the pristine tube occurs around 1.9 eV. However, the adsorption of surface Li atoms incurs absorption also in the low-energy region in some cases.

For each type of tube, in general, the RBM frequencies are reduced because of the dilation of the diameter of the optimized tube except for the case of two surface Li atoms on the optimized (3, 3) nanotube, where an enhancement of 2% is observed.

Acknowledgments

The authors express thanks to the University Grants Commissions, New Delhi for financial assistance and to Dr P S Yadav for providing us with the computation facilities.

References

Agrawal B K *et al* 2003 *J. Phys.: Condens. Matter* **15** 6931
Baughman R H, Zakhidov A A and de Heer W A 2002 *Science* **297** 787
Bendiab N *et al* 2001 *Phys. Rev.* B **64** 245424
Collins P G *et al* 2002 *Science* **287** 1801
Farajian A A *et al* 2003 *Phys. Rev.* B **67** 205423
Fuchs M and Scheffler M 1999 *Comput. Phys. Commun.* **119** 67
Goedecker S 1997 *SIAM J. Sci. Comput.* **18** 1605
Gonze X 1996 *Phys. Rev.* B **54** 4383
Hirscher M *et al* 2002 *J. Alloys Compounds* **330** 654
Hybertson M S and Needles M 1993 *Phys. Rev.* B **48** 4608
Jorio A *et al* 2002 *Chem. Phys. Lett.* **351** 27
Kleinman L and Bylander D M 1982 *Phys. Rev. Lett.* **48** 1425
Kong J *et al* 2000 *Science* **287** 622
Launois P *et al* 2000 *Solid State Commun.* **116** 99
Liang W *et al* 2002 *Appl. Phys. Lett.* **80** 3415
Lie Z M *et al* 2001 *Phys. Rev. Lett.* **87** 127401
Liu H J and Chan C T 2003 *Solid State Commun.* **125** 77
Machon M *et al* 2002 *Phys. Rev.* B **66** 155410
Moli Z *et al* 2001 *Phys. Rev. Lett.* **87** 127401
Ouyang M *et al* 2001 *Science* **292** 702
Payne M C *et al* 1992 *Rev. Mod. Phys.* **64** 1045

Perdew J P, Burke K and Ernzerhof M 1996 *Phys. Rev. Lett.* **77** 3865
Qin L C *et al* 2000 *Nature* **408** 50
Qiu S *et al* 1989 *Zeolites* **9** 440
Saito Y *et al* 2002 *Mol. Cryst. Liq. Cryst.* **387** 303
Schlapbach M and Zuttel M 2001 *Nature* **414** 353
Shim M *et al* 2002 *Nano Lett.* **2** 285
Shimoda H *et al* 2002 *Phys. Rev. Lett.* **88** 015502
Sumanasekera G U *et al* 2000 *Phys. Rev. Lett.* **85** 1096
Sun H D *et al* 1999 *Solid State Commun.* **109** 365
Tang Z K *et al* 1998 *Appl. Phys. Lett.* **73** 2287
Tang Z K *et al* 2001 *Science* **292** 2462
Troullier N and Martins J L 1991 *Phys. Rev.* B **43** 1993
Tu Z and Ou-Yang Z 2002 *Phys. Rev.* B **65** 233407 and the references cited therein
Wang N *et al* 2000 *Nature* **408** 50
Ye J T *et al* 2003 *Phys. Rev.* B **67** 113404
Yoon Y G, Delaney P and Louie S G 2002 *Phys. Rev.* B **66** 073407
Zhao J *et al* 2000 *Phys. Rev. Lett.* **85** 1706

INSTITUTE OF PHYSICS PUBLISHING JOURNAL OF PHYSICS: CONDENSED MATTER

J. Phys.: Condens. Matter **18** (2006) 10115 doi:10.1088/0953-8984/18/40/C01

Erratum

An *ab initio* study of optical and Raman spectra of heavily Li-doped 4 Å carbon nanotubes

Professor B K Agrawal 2006 *J. Phys.: Condens. Matter* **16** 1467–1488

Our corrected cohesive energy for the bulk Li is in fact 1.82 eV (in contrast to the value reported in the paper, 0.5 eV) against the experimental value of 1.63 eV. When the binding energies are now calculated after taking the bulk Li energy as the reference energy, the calculated binding energies turn out to be more or less in agreement with the values of Liu and Chan [1]. The authors apologise to Liu and Chen for the unfounded criticism of their work in the paper.

None of the results of the above paper depends upon the bulk Li energy and therefore our results for the binding energies presented in the various tables which have been obtained after taking the isolated Li atom energy as the reference energy remain unaffected. Thus all the results for the binding energies, electronic structure, optical absorption and Raman active radial breathing mode frequencies obtained are technically sound and free from error.

References

[1] Liu H J and Chan C T 2003 *Solid State Commun.* **125** 77

0953-8984/06/4010115+01$30.00